JOURNAL OF GEOPHYSICAL RESEARCH, VOL. 104, NO. D17, PAGES 21,707–21,717, SEPTEMBER 20, 1999

O_3 oxidation of SO_2 in sea-salt aerosol water: Size distribution of non-sea-salt sulfate during the First Aerosol Characterization Experiment (ACE 1)

H. Sievering[1], B. Lerner, and J. Slavich
Global Change and Environmental Quality Program and Department of Environmental Sciences and Geography, University of Colorado at Denver

J. Anderson and M. Posfai
Department of Geology and Chemistry, Arizona State University, Tempe

J. Cainey
CSIRO, Atmospheric Research, Aspendale, Victoria, Australia

Abstract. Non sea-salt sulfate (NSS) of 2.2-2.3 nmol m^{-3} total magnitude in aerosols observed during the First Aerosol Characterization Experiment (ACE-1) at Cape Grim, Tasmania, was trimodally distributed with ~1 nmol NSS m^{-3} in >0.7 μm ambient diameter (diam) coarse sea-salt mode aerosols; despite this low NSS concentration, $[H_2SO_4(g)]$ was so low that <1% of this NSS could have been due to H_2SO_4 scavenging. Ammonium was not associated with these coarse sea-salt aerosols, suggesting that cloud processing was a minor contributor to the NSS found in >0.7 μm diam aerosols. The mechanism of O_3 oxidation of SO_2 in sea-salt aerosol water (SSAW) is assessed for its capability to explain this coarse aerosol NSS. Limitation of this mechanism's NSS contribution is largely due to SSAW's buffering capacity since its reaction rate is reduced by 2 orders of magnitude at pH 6 versus the $p\text{H} \geq 8$ of unreacted SSAW. However, the buffering capacity of sea-salt aerosols may have been significantly enhanced over that of bulk seawater alkalinity. This appears to be due to carbonate resulting from small fragments of biogenic $CaCO_3$ in the ocean's surface microlayer. Given the observed nonsoil calcium excess over that in bulk seawater, the estimated actual buffering capacity of sea-salt aerosols observed during ACE 1 was 50%, or more, enhanced over that due to bulk seawater alkalinity. Considering this enhanced buffering capacity, O_3 oxidation of SO_2 in SSAW can produce sufficient NSS to explain 70-90% of the ~1 nmol m^{-3} found in >0.7 μm diam coarse sea-salt aerosols with cloud processing and further oxidation of SO_2 in SSAW (i.e., $p\text{H} < 6$) by other sea-salt conversion mechanisms contributing the remainder. The amount of NSS produced by sea-salt conversion mechanisms during the ACE 1 remote Southern Ocean experiment vied with homogeneous and cloud processing in their contribution to the total observed NSS of 2.2-2.3 nmol m^{-3}.

1. Introduction

Observations of the size distribution of non sea-salt sulfate (NSS) within the global marine boundary layer (MBL) have shown that a substantial fraction of it is found in >1 μm ambient diam, predominantly sea-salt aerosols [*Gravenhorst*, 1978; *Sievering* et al., 1990; *Prospero and Savoie*, 1993]. These large aerosols have high dry deposition rates with removal of sulfur to the ocean's surface waters an important consideration in MBL sulfur budgets. Depending on the sampling efficiency of sea-salt aerosols and meteorological as well as pollution conditions (locally and upwind), the observed NSS found in these large aerosols may vary from an indeterminable amount to 5 nmol NSS m^{-3}, and more. The percentage of total aerosol NSS that this constitutes has been observed to be less than 10% (polluted conditions) to 30% and more (unpolluted conditions) over the North Atlantic Ocean [*Sievering et al.*, 1995]. High wind speed conditions, supporting the strong production of sea-salt aerosols, have been shown to enhance this percentage [*Sievering et al.*, 1990, 1992].

Modeling of the MBL sulfur cycle [*Luria and Sievering*, 1991; *Chameides and Stelson*, 1992] shows that multiphase SO_2 conversion in sea-salt aerosols can explain much of the observed sea-salt aerosol NSS. This mechanism relies on the oxidation of aqueous phase sulfur, S(IV), in the high pH water associated with sea-salt aerosols, hereafter referred to as sea-salt

---

[1] Also at Aerosols Group, Climate Monitoring and Diagnostics Laboratory, NOAA, Boulder, Colorado.

Paper number 1998JD100086.
0148-0227/99/1998JD100086$09.00

aerosol water (SSAW). Under typical wind speed and relative humidity MBL conditions, 75-90% of the sea-salt aerosol volume is water [e.g., *Kim et al.*, 1990] of *p*H 8 or more upon emission from the ocean's surface, and of *p*H 6-8 in the lowest tens of meters of the MBL [*Winkler*, 1986]. This high *p*H water supports the rapid oxidation of S(IV) by O_3 in SSAW; mass-transfer resistance of SO_2 and O_3 into the SSAW may contribute to its limitation in some circumstances [*Chameides and Stelson*, 1992; *Sievering et al.*, 1992].

The remote, clean air MBL contains [SO_2] <100 parts per trillion by volume (pptv) resulting, largely, from dimethylsulfide (DMS) emissions at the ocean's surface [*Warneck*, 1988]. Understanding of the global sulfur cycle must include multiphase SO_2 conversion such as O_3 oxidation of SO_2 in SSAW makes to the observed NSS in remote areas of the MBL. The First Aerosol Characterization Experiment (ACE 1), provided an opportunity to do this in the cleanest, most remote area of the MBL. This area is the Southern Ocean southwest of Tasmania during extremely long ocean fetch conditions encountered in November and December. Under these conditions, total aerosol NSS is very low [*Berresheim et al.*, 1990], less than half the lowest values observed over the North Atlantic of about 7 nmol NSS m^{-3} [*Sievering et al.*, 1995]. During this time of year, wind speeds in the Southern Ocean's MBL are typically >8 m s^{-1} [*Jasper and Downey*, 1990; *Downey and Jasper*, 1996]. Thus extremely clean MBL air with high sea-salt aerosol concentrations was expected during ACE 1, November and December 1995. The purpose of this paper is to describe the size distribution of NSS found during ACE 1 and to estimate the contribution of O_3 oxidation of SO_2 in SSAW to this observed NSS.

2. Experiment

Atmospheric sampling was conducted at two locations: the Cape Grim Baseline Air Pollution Station (40°, 41'S; 144°, 41'E) at the northwestern tip of Tasmania and on board the National Oceanic and Atmospheric Administration (NOAA) ship *Discoverer*. A six-stage high-volume (1130 liter per min (Lpm)) cascade impactor (Graseby-Anderson, Smyrna, Georgia) which efficiently samples 0.1 to 12-22 μm (depending on wind speed and direction relative to sampler [*Wedding et al.*, 1977]) ambient diam aerosols, was installed at the 50-m level on the sampling tower at Cape Grim, placing it well above the ground and clear of any local soil inputs (J. Anderson, personal communication, June 1997). This also placed the high-volume impactor well above local sea spray influences which may be significant at lower levels on the sampling tower as a result of the 90 m bluff at the sea's edge upon which the Cape Grim station sits. Detailed wind tunnel studies of the Cape Grim site [*Baines and Murray*, 1992] show the 50-m sampling tower level (at 140-m physical height above sea level [asl]) to be at 110-130 m effective asl (depending on wind speed and direction) due to compression effects as air moves up over the bluff. A second high-volume cascade impactor was installed at the 30-m tower level to assess whether local soil and sea spray influences were present at this level. Criteria for the sampling of very clean marine air at Cape Grim (hereafter referred to as clean MBL air), based on more than a decade of sampling, 190°-280° wind direction sector and <1200 cm^{-3} condensation nuclei (CN) count, were used to control high-volume airflow on and off modes. All samples considered here were obtained under clean MBL air conditions. Obtaining these clean MBL air conditions caused actual sampling times to be 30-35% of total exposure times. Thus day versus night sampling was not possible. Such sampling previously showed [*Sievering et al.*, 1991, 1995] no statistical difference in the observed day versus night sea-salt aerosol NSS.

Sampling on board the NOAA ship *Discoverer* took place from the deck of the flying bridge since all sampling locations closer to the ship's bow were occupied by other ACE 1 aerosol and gas sampling instrumentation. Condensation nuclei (CN) counter (courtesy of T. Carsey, NOAA-AOML, Miami, Florida) and SO_2 monitor [*De Bruyn et al.*, 1998] inlets were colocated with a high-volume cascade impactor on the flying bridge. Data from these samplers were used to determine which cascade impactor samples may have been contaminated by the ship's stack effluent. Only three impactor samples were found to be contaminated during ship transit sampling; that is during the mid-October to mid-November transit from Seattle in the United States to Hobart, Tasmania. However, most of the ACE 1 intensive Southern Ocean high-volume impactor samples were designated as contaminated.

Whatman 41 high-volume impactor filters were changed in the Cape Grim and *Discoverer* laminar flow boxes. Sample filters were stored frozen until preparation for analysis. Three filter impaction strips (from 10 total strips) were used in Dionex ion chromatography analyses, both at the Center for Environmental Sciences of the University of Colorado at Denver and at the Australian Government Analytical Laboratory in Hobart, Tasmania. Filter impaction strips were placed in vials, covered with 6 mL deionized water and sonicated. Concentrations of Na^+, K^+, NH_4^+, Ca^{++}, Mg^{++}, Cl^-, NO_3^-, $SO_4^=$, and MSA were determined.

A 12-stage micro-orifice uniform deposit cascade impactor (Moudi-MSP Corp., Minneapolis, Minnesota) was also used [*Cainey*, 1997]. The Moudi efficiently sampled particles (about 95%) at 30 L min^{-1} in the 10 to 0.1 μm diam size range using 47 mm, 0.04 μm pore-sized filters as the collection substrate on the 11 impactor stages; a 37 mm, 0.4 μm pore-sized filter acted as the final stage. Ambient air was brought to a relative humidity < 50% before sampling by heating the incoming air stream to 30°C. Samples obtained over 1- to 2-week periods commenced in September 1993 and terminated in April 1996 to provide the determination of seasonal variations in the NSS size distribution. Analysis of the exposed filters was by suppressed ion chromatography after extraction in 5 mL of deionized water. Dionex CS12 analytical and CG12 guard columns were used in the manner described by the manufacturer (document #034657) for the determination of low NH_4^+ in the presence of high Na^+ concentrations. The Moudi and Sierra impactors complement each other in that Moudi <1 μm data are better defined, whereas Sierra impactor >1 μm data are better defined.

Sampling for individual particle analysis by scanning and transmission electron microscopy analysis (see *Posfai et al.*, [1995] on this type of analysis) was colocated with and in time sequence with the cascade impactor sampling at the 50-m Cape Grim tower level. Meteorological data were also collected at this level. Ancillary aerosol and gas data (including SO_2 and O_3), obtained throughout all cascade impactor sampling, are described elsewhere in this special ACE 1 issue.

3. Results

An overview of meteorological and sample time conditions during the Cape Grim ACE 1 intensive is shown in Figure 1.

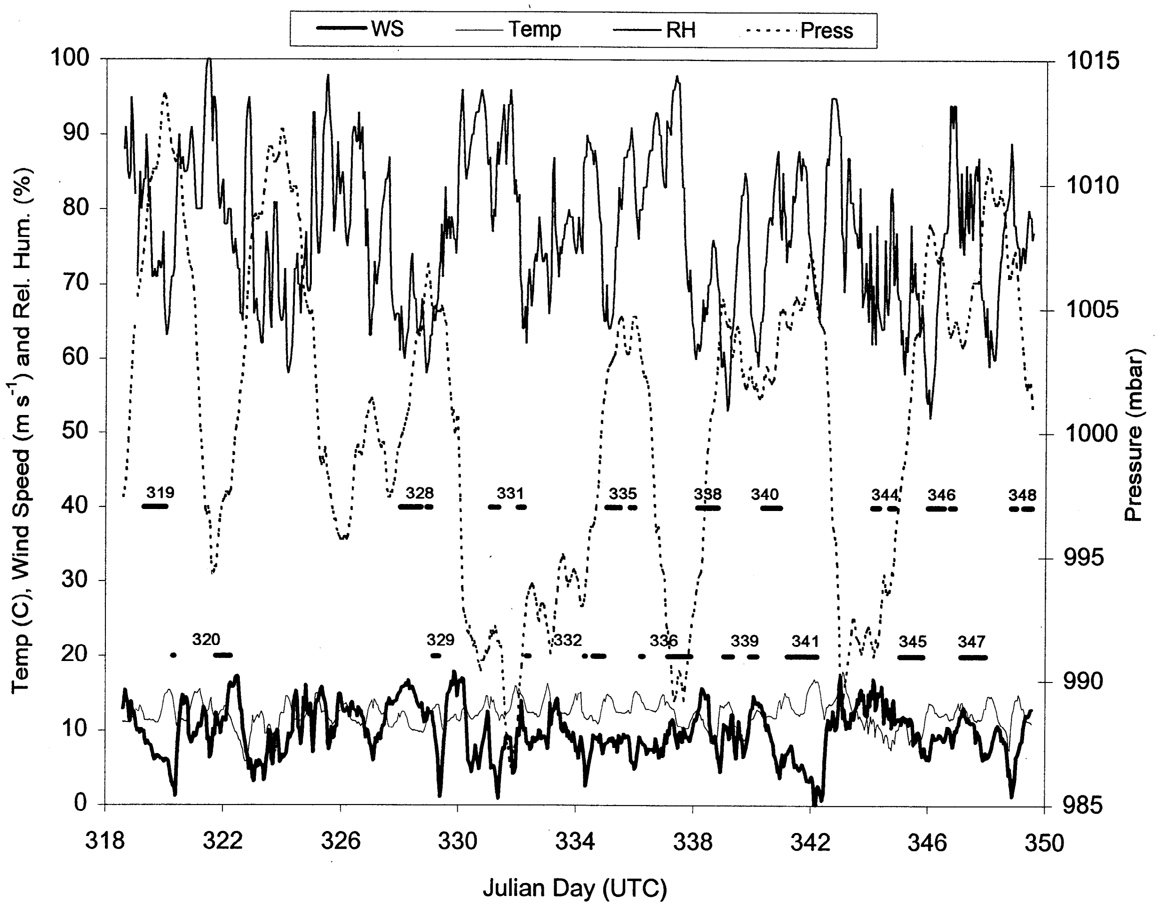

Figure 1. Meteorological and sample time conditions during the entire ACE 1 Cape Grim intensive program.

An overview of the Cape Grim cascade impactor ion size distribution results during ACE 1 is found in Tables 1 (high-volume impactor) and 2a (Moudi impactor). Presented here are average ion concentrations, in nmol m^{-3}, across the entire month-long ACE 1 period for three size classifications: a coarse fraction dominated by sea-salt aerosols and chemical processes which occurred therein: a fine fraction influenced by both sea-salt and accumulation mode aerosols; and a very fine fraction dominated by the accumulation mode but also influenced by the Aitken mode. For the high-volume impactor, coarse includes the >0.9 μm ambient diam (all stated diameters are for ambient air conditions) aerosols and is a sum of data from Sierra impactor stages 1 through 4, fine includes 0.4-0.9 μm diam aerosols (stage 5), and very fine is <0.4 μm diam (backup stage). For the Moudi impactor an ambient/dried diam growth factor was applied, 1.7 for coarse, 1.5 for fine, and 1.3 for very fine, resulting in coarse, fine, and very fine ambient diam size ranges of >0.7 μm (Moudi stages 1 through 6), 0.35-0.7 μm (stage 7), and <0.35 μm (stages 8-11), respectively. (Sample-by-sample results are archived by the UCAR Joint Office for Science Support and are found at http://www.joss.ucar.edu/codiac/.)

Several aspects of the Table 1 and 2a results may be highlighted:

Table 1. ACE 1 Average (n = 17) Coarse, Fine, and Very Fine Ion Concentrations Obtained by the High-Volume Impactor at 110-130 m Effective asl During Clean MBL Conditions at Cape Grim

Ambient Diam μm	Na^+	Alk.	NH_4^+	Ca^{2+}	Mg^{2+}	SO_4^{2-}	Cl^-	NO_3^-	MSA	Cl_{def}	NSS
>0.9	169.4 (39.6)	0.85 (0.21)	<0.1 (0.05)	4.09 (0.91)	19.1 (4.6)	10.9 (2.2)	201.5 (46.9)	0.47 (0.18)	0.23 (0.05)	-7.5 (2.6)	0.84 (0.13)
0.4 to 0.9	2.3 (0.8)	0.013 (0.004)	0.34 (0.15)	0.10 (0.03)	0.26 (0.07)	0.59 (0.06)	3.0 (1.0)	0.05 (0.02)	0.10 (0.02)	-0.2 (0.54)	0.44 (0.07)
<0.4	0.71 (0.29)	0.004 (0.002)	2.17 (0.54)	0.08 (0.03)	0.05 (0.01)	1.01 (0.13)	0.54 (0.43)	0.004 (0.011)	0.17 (0.02)	0.1 (0.21)	0.97 (0.13)

Values in parentheses are the 95% confidence intervals about the means. The NSS values are the average of each sample's $[SO_4^{2-}] - 0.063[Na^+]$. All concentrations in nmol m^{-3}.

Table 2a. ACE 1 Average (n = 4) Coarse, Fine, and Very Fine Ion Concentrations Obtained by the Moudi Impactor at 30-40 m Effective asl During Clean MBL Conditions at Cape Grim [Cainey, 1997]. All concentrations in nmol m^{-3}.

Ambient Diam µm	NH_4^+	Ca^{++}	Mg^{++}	$SO_4^=$	Cl^-	NO_3^-	Cl_{def}	NSS
>0.7	<0.0	2.34	10.2	6.4	120.4	0.67	~-13	1.02
.35–.7	0.21	0.03	0.09	0.4	0.47	0.10	~0.5	0.35
<0.35	1.72	0.06	0.14	0.9	0.93	0.14	~0.4	0.90

Table 2b. Seasonal Average (n = 13-23 for Each Season; Spring is September, October, and November) Coarse, Fine, and Very Fine Mode Mg-Based NSS. Obtained by Inversion of the Moudi Impactor Data During Clean MBL Conditions at Cape Grim [Cainey, 1997]

Mode	Spring	Summer	Fall	Winter
Coarse	1.26	1.20	0.91	1.48
Fine	0.63	1.73	0.78	0.34
Very Fine	0.24	0.29	0.09	0.04
Total	2.12	3.21	1.77	1.86

Mode size cuts depend on season; very fine upper cut is 0.1-0.15 µm ambient diam range, and fine upper cut is 1.0-1.5 µm diam range. Units are nmol m^{-3}.

1. The average calculated NSS ($SO_4^=$ - 0.0603 Na^+), summed across all size ranges, is 2.3 nmol m^{-3}, very low in comparison to our previous North Atlantic observations [*Sievering et al.*, 1995].
2. NSS is largely bimodal in character with 0.9-1 nmol m^{-3} of NSS found in both coarse and fine aerosols; the Moudi impactor indicated that a minor NSS Aitken mode mass was also present.
3. No NH_4^+ or calculated chloride deficit ($Cl_{def} = 1.165\ Na^+ - Cl^-$) is found for coarse sea-salt aerosols, distinctly different from North Atlantic observations.
4. In fine aerosols, the amount of Na^+ is substantially greater than NH_4^+, with NSS slightly greater than NH_4^+ (molar basis).
5. The coarse aerosol alkalinity (Alk., calculated as 0.005 Na^+) is about half (equivalence basis) of the NSS found in coarse sea-salt aerosols.

Table 2b shows the seasonal variation of NSS in each of the coarse, fine, and very fine aerosol modes determined by inversion of the Moudi impactor data (mode upper cuts are here defined by inversion calculations; they are 0.1-0.15 µm for very fine and 1-1.5 µm for fine, depending upon season [*Cainey*, 1997]). Note that more than half of the NSS, except for the summer season, is found in the coarse sea-salt mode and that this coarse NSS in the winter season is fully 80% (1.48 nmol m^{-3})of the total NSS observed.

Meteorological conditions at Cape Grim during ACE 1 were typical for November and December with high wind speeds of 7 to 16 m s^{-1} (average of 10.4 m s^{-1}) and relative humidity (RH) of low variability, 76±6%, prevailing. Concentrations of the relevant gaseous species for the consideration of O_3 oxidation in SSAW, such as SO_2, O_3, H_2O_2, HNO_3, and NH_3, are discussed elsewhere in this special issue on ACE 1. Here we note only that both SO_2 and NH_3 concentrations were quite low, 5 pptv to 40 pptv, throughout ACE 1 and that sample-averaged O_3 varied from 15 ppbv to 30 ppbv, except for one outlier of 70 ppbv. H_2O_2 was 0.5-1 ppbv throughout. Presumably, HNO_3 was very low since aerosol NO_3^- concentrations were <1 nmol m^{-3}.

Results from ship low-volume impactor sampling indicate slightly lower total NSS of 2.0-2.1 nmol m^{-3} during Southern Ocean sampling south and southwest of Cape Grim [*Quinn et al.*, 1998]. Wind speeds were slightly lower than at Cape Grim with average Na^+ about 80% of the amount shown in Table 1. Shipboard sampling was at 16-18 m asl versus the 110-130 m asl sampling at Cape Grim. The ship NSS data only occasionally displayed a bimodal character; 0.9-1.0 nmol NSS m^{-3} was found in aerosols >0.8 µm ambient diam. Results from high-volume impactor sampling aboard the ship during a part of the transit from Seattle to Hobart (30°S-40°S; 160°W-155°E) are shown in Table 3 along with further results from the Cape Grim high-volume impactor sampling.

4. Discussion

The O_3 oxidation of SO_2 in SSAW is known to occur at a rapid rate [*Chameides and Stelson*, 1992; *Sievering et al.*, 1991]. However, the production of NSS by this mechanism is quenched once the buffering capacity of SSAW is consumed, since the *p*H of SSAW has then dropped from 8 or more to 6 or less. At a *p*H of 6, O_3 oxidation of SO_2 in SSAW is slowed by 2 orders of magnitude to a rate less than or equal to that of H_2O_2 in SSAW. Thus the major contribution to NSS by the O_3 oxidation pathway is essentially complete within 10-20 min

Table 3. ACE 1 Average Coarse, Fine, and Very Fine Non-Sea-Salt Sulfate (NSS) and Excess Ca^{++}(CaX) Equivalence Concentrations Obtained by the High-Volume Impactor at 110-130 m asl During Clean MBL Conditions at Cape Grim and at 16-18 m asl During South Pacific *Discoverer* Ship Transit Sampling. Concentrations in neq m^{-3}.

Ambient Diam µm	NSS	CaX
	Cape Grim	
> 0.9	1.69(±0.47)	0.72(±0.035)
0.4 to 0.9	0.89(±0.13)	0.10(±0.04)
<0.4	1.94(±0.15)	0.10(±0.03)
	Ship Transit (30°S-40°S, 160°W-155°E)	
>0.9	3.32	1.68
0.4 to 0.9	2.40	0.11
<0.4	1.85	0.02

[*Chameides and Stelson*, 1992]. Thereafter, the H_2O_2 oxidation pathway and/or other multiphase pathways [*Keene et al.* (1998); *Vogt et al.*, 1996], having been activated by O_3 oxidation's influence on SSAW pH, continue to produce NSS throughout the remainder of the sea-salt aerosol's lifetime.

The additional NSS produced by O_3 oxidation during the sea-salt aerosol's lifetime is less than 20% beyond its contribution in the first tens of minutes [*Chameides and Stelson*, 1992]. It is therefore of interest to look more closely at the NSS in and buffering capacity of coarse sea-salt aerosols observed during ACE 1.

The buffering capacity accompanying the sea-salt aerosol as it is emitted from the sea surface is generally seen as equal to its bicarbonate/carbonate plus borate alkalinity. Assuming for the moment that the sea-salt aerosol's alkalinity to Na^+ ratio remains the same as that for bulk seawater (Alk. represents this alkalinity in Table 1), the average ratio of NSS to Alk. (equivalence basis) in >0.9 μm coarse sea-salt aerosols at Cape Grim is, then, 2.0 with a 90% confidence interval (CI) of ±0.6. A similar result was observed by *Quinn et al.* [1998] aboard the *Discoverer*. Given that the O_3 oxidation pathway may contribute only 20% more to NSS production once SSAW's buffering capacity is lost, only up to half of the coarse sea-salt aerosol's NSS is thereby explained..

Aerosol alkalinity (A Alk) may be somewhat greater than bulk seawater derived alkalinity (Alk.) due to thermodynamic equilibrium between CO_2 (gas) and CO_2 (aq) and the resulting shift in the $[HCO^-_3]/[CO_3^=]$ ratio as the sea-salt aerosol evolves and water evaporates. Using *Millero's* [1995] thermodynamic equilibrium constants, and noting that the dissolved solids in sea-salt aerosols at 80% RH are approximately 7 times more concentrated than in bulk seawater, a modeling analysis (P. Tans, personal communication, June 1997) of dissolved inorganic carbon in unreacted sea-salt aerosols was undertaken. At 20°C the $[HCO_3^-]/[CO_3^=]$ ratio was found to be 3.2 in sea-salt aerosols at 80% RH, whereas this ratio is 13.4 in bulk seawater. For typical RH and temperatures within the MBL it appears A Alk may be enhanced (5-20%) over that of Alk. This increases the portion of >0.9 μm coarse aerosol NSS that can be explained by the O_3 oxidation pathway to about half.

The contribution of cloud processing to the coarse aerosol NSS must be considered. A number of studies regarding the effect clouds have on the aerosol size distribution [e.g., *Hoppel et al.*, 1994] do not show any super-micron aerosols resulting. Figure 2 shows the average Moudi 12-stage impactor size distribution for NSS and NH_4^+ observed by *Cainey* [1997] during ACE 1 at Cape Grim. The accumulation mode is clearly present, though it is a narrower mode (and all below 1 μm diam) than found in the MBL over the North Atlantic [*Kim et al.*, 1995]. The contrast between the NSS and NH_4^+ size distributions is particularly noteworthy. As Table 2a indicates, <0.03 nmol NH_4^+ m^{-3} was found in >0.7 μm aerosols using the Dionex CS12 column "low NH_4^+ in the presence of high Na^+" IC procedure. Yet, in the 0.2-0.35 μm size range, where the accumulation mode peaks, NH_4^+ nearly equals NSS, on an equivalence basis, indicating that accumulation mode NSS is largely present as $(NH_4)_2SO_4$. This was also found over the Southern Ocean generally using aircraft sampling [*Berresheim et al.*, 1990]. Despite ammonium sulfate dominating the very fine (<0.35 μm) size fraction, essentially no NH_4^+ was found in >0.7 μm coarse sea-salt aerosols (the ratio of very fine NH_4^+ to coarse NH_4^+ is 100 or more). Thus the physical mechanisms of collision-coalescence cloud processing and coagulation together could not have contributed more than about 1% to the coarse aerosol NSS. Scavenging of gaseous H_2SO_4 was not a significant contributor to coarse aerosol NSS since daily averaged $[H_2SO_4]$ was <0.1 pptv (F. Eisele, personal communication, October 1997) or <1% of the observed $[SO_2]$ of 14 pptv [*De Bruyn et al.*, 1998].

Sea-salt aerosols may themselves act as cloud condensation nuclei with SO_2 oxidation proceeding in the resulting cloud droplets [*Noone et al.*, 1996]. This in-cloud production of NSS may generate sulfate in coarse sea-salt aerosols [*Ayers and Larson*, 1990; *Lowe et al.*, 1996]. Such NSS production is accompanied by the production of NH_4^+, since ammonia is readily scavenged by the relatively low *p*H cloud water accumulating on sea-salt nuclei [*Ayers and Larson*, 1990]. When sea-salt aerosol alkalinity is available, ammonia scavenging may be reduced. However, as shown above, alkalinity is rapidly consumed (10-30 min) after emission from the sea surface. These aerosols, acting as nuclei at cloud base, should have little or no buffering capacity left to neutralize NSS produced in cloud. Thus ammonium sulfates should be produced by SO_2 oxidation in cloud droplets growing on sea-salt nuclei as long as there is any NH_3 present. *Ayers and Larson* [1990] indicate that $[NH_3]$ is likely to be ~30 pptv at cloud base in the Southern Ocean's atmosphere; *Ayers and Gras* [1983] observed an average of 80 pptv at Cape Grim with no seasonality present. The ACE 1 NH_3 aircraft observations [*Davis,* 1997] indicate 40-200 pptv of NH_3 was present in the Southern Ocean's MBL.

Gurciullo et al. [this issue] used a sized-resolved chemistry and cloud microphysics model with $[SO_2]$ of 8-22 pptv and the conservatively low $[NH_3]$ of 15-50 pptv, along with the size-distributed aerosol ion data of Table 1, as modeling constraints. They investigated the size distribution of cloud produced sulfate for ACE 1 conditions, but their simulation results can also be used to estimate how much NH_4^+ may be associated with coarse, sea-salt aerosol due to cloud processing. Assuming $[SO_2]$ of 14 pptv, the cloud model produced 25-45% of the NSS actually observed in the >0.9 μm size range but also produced 0.2 nmol m^{-3} of NH_4^+ in this range. This result assumed that most of the sea-derived alkalinity (Alk.), 0.85 nmol m^{-3}, was available upon ingestion into cloud. Recall that very little, if any, sea-salt aerosol buffering capacity is likely to remain within these aerosols by the time they are at cloud base. The 0.2 nmol NH_4^+ m^{-3} may be compared with <0.03 nmol NH_4^+ m^{-3} observed to be present in >0.7 μm aerosols during ACE 1. To retrofit coarse aerosol $[NH_4^+]$ <0.03 nmol m^{-3}, as observed, drives the coarse aerosol NSS produced by in-cloud processing to <10% of that observed.

In-cloud chemical processing appears to explain only a minor fraction of the coarse aerosol NSS so we reconsider the buffering capacity of sea-salt aerosols. This since O_3 oxidation of SO_2 in SSAW will produce more NSS if a greater buffering capacity is available. Examination of the ion data obtained by high-volume impactor sampling (Table 1) indicates a Ca^{++} excess, CaX, prevailed over that due to bulk seawater (CaX = Ca^{++} - 0.022 Na^+). Others have reported CaX excesses in sea-salt aerosols [e.g., *Junge*, 1972; *MacIntyre*, 1974; *Duce and Hoffman*, 1976; *Cattell et al.*, 1977]. The average CaX observed at Cape Grim was 0.38 nmol m^{-3} for coarse aerosols, and 0.05 nmol m^{-3} for both the fine and very fine aerosols. Considering all six stages of the high-volume impactor, the ratio of Ca^{++} to bulk seawater derived Ca^{++} increases with decreasing size of aerosols: 1.1 for >8 μm; 1.1 for 4.5-8 μm; 1.2 for 2.3-4.5 μm; 1.4 for 0.9-2.3 μm; 2.8 for 0.4-0.9 μm; and 3.3 for <0.4

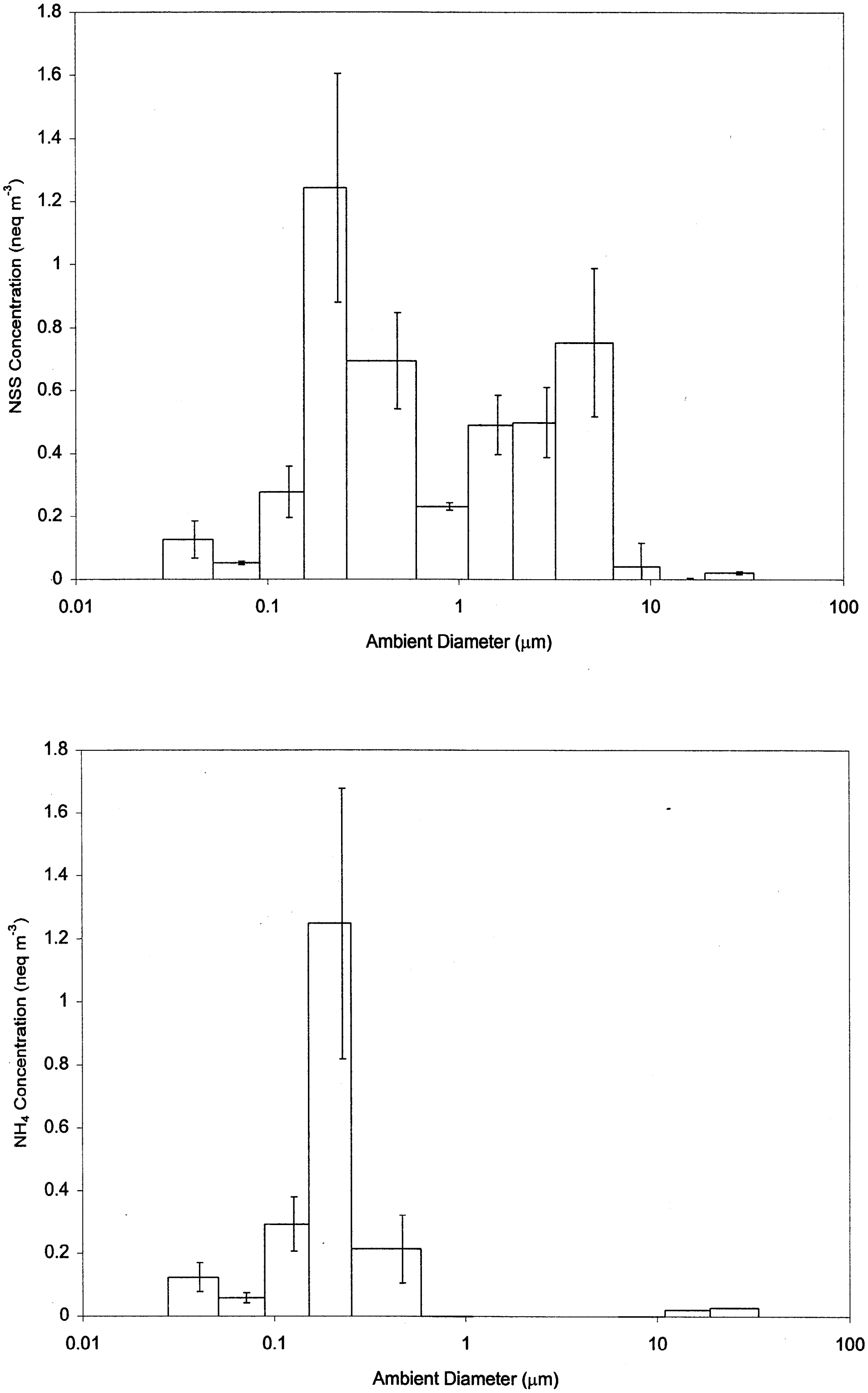

Figure 2. ACE 1 average NSS and NH_4^+ (in neq m^{-3}) obtained by the Moudi impactor as a function of 12 aerosol size cuts during clean MBL conditions at Cape Grim [*Cainey et al.*, 1997]. Error bars represent standard deviation about each mean.

μm diam aerosols (B. Lerner et al., unpublished manuscript, 1998). The Moudi impactor results indicate a ratio of about 2.4 for the <0.7 μm diam aerosols. Aircraft measurements by *Cattell et al.* [1977], sampling Southern Ocean derived air over and upwind of Tasmania, observed a ratio of 2.4 (± 0.5) for >1 μm diam aerosols. *Maenhaut et al.* [1983] found the Ca^{++} to bulk seawater derived Ca^{++} ratio to be 1.31, 1.57, and 1.82 for the >4, 2-4, and 1-2 μm diam ranges, respectively, in a suite of Pacific Ocean MBL samples removed from soil input. *Artaxo et al.* [1992] observed this ratio over the Weddell Sea to be 1.33 for 2-15 μm and 1.53 for <2 μm diam aerosols.

The aerosol size dependent enhancement of Ca^{++} can be explained as originating from the sea-salt aerosol production process at the air-sea interface. Bursting bubbles are the major source of sea-salt aerosols. They efficiently skim the sea surface microlayer, which often has a composition different from that of bulk seawater (e.g., *Hoffman and Duce* [1976]. *MacIntyre* [1974] reviewed the physical mechanisms which may explain the enhancement of ionic species at the air-sea interface. He indicated that binding to organic molecules is a contributor and that divalent cations such as Ca^{++} and Mg^{++} are more strongly bound than monovalent ions. MacIntyre also indicated that small biogenic $CaCO_3$ skeletal fragments concentrate in the surface microlayer; these may lead to both Ca^{++} and $CO_3^=$ enhancement in the microlayer. It is known that the first jet drop as well as most film drops produced by bursting bubbles are endowed with this surface microlayer material [*Warneck*, 1988]. Film drops have a broad distribution with a maximum at 0.3-0.5 μm diam, depending on relative humidity, whereas jet drops also are broadly distributed with a maximum at 3-4 μm diam [*O'Dowd et al.*, 1997]. Thus it may be expected that CaX increases with decreasing size as observed at Cape Grim. The smaller the $CaCO_3$ fragments are, the more soluble they are likely to be in surface microlayer seawater [*Henrichs and Williams*, 1985]. Further, small seawater bubbles have been found to be more effective in transporting sea surface microlayer material into the air [*Bezdek and Carlucci*, 1974; *Tseng et al* 1992].

Table 3 shows (in neq m^{-3}) a comparison of average coarse, fine, and very fine NSS with CaX for both Cape Grim and ship transit sampling, the latter for cases (n=10) removed from continental input. The coarse CaX of 0.72 neq m^{-3} (Cape Grim) represents an ~ 10% excess over bulk seawater derived Ca^{++}, whereas the CaX of 1.68 neq m^{-3} (ship transit) represents a 20-25% excess. The latter CaX implies that actual coarse aerosol SSAW buffering capacity may have been as much as 2.5 times that of bulk seawater derived alkalinity alone.

Regression analysis of NSS versus all other ion data across the ACE 1 experiment showed it to be most strongly dependent upon Alk., the aerosol alkalinity based upon bulk seawater alkalinity. For a regression including all aerosol size ranges, the result is

$$\mathrm{NSS} = 0.034 + 1.92\,[\mathrm{Alk.}] + 0.47\,[\mathrm{NH_4^+}] \qquad (1a)$$

with $p < 0.0001$ for both Alk. and NH_4^+, $p = 0.0529$ for the intercept, and $R^2 = 0.80$ (F ratio = 96.1). For a regression including only the coarse aerosol data (i.e., >0.7 μm diam where no NH_4^+ was present), the result is

$$\mathrm{NSS} = 0.014 + 2.08\,[\mathrm{Alk.}] \qquad (1b)$$

with $p < 0.0001$ for Alk. and $p = 0.4592$ for the intercept, and $R^2 = 0.82$ (F ratio = 105.7). The Alk. regression coefficient in both equations calls for a buffering capacity which is about twice that based upon bulk seawater alkalinity. The coarse aerosol intercept in equation (1b) is not significant, indicating that there is a direct linear correlation between alkalinity and NSS. *Chameides and Stelson* [1992] noted that a linear relationship between alkalinity and NSS would exist in coarse aerosol only until the initial buffering capacity of the aerosol (with the initial SSAW *p*H near 8) was consumed. *Cainey* [1997] found that the >0.7 μm diam aerosol was alkaline relative to smaller aerosol; however, only a small *p*H data set was obtained, so it is difficult to state the range of *p*H which prevailed throughout ACE 1 over any size range. Alternatively, when NSS is correlated over the entire aerosol size range, NH_4^+ enters into the regression (as ammonium sulfate in the fine aerosol), and the intercept becomes much more significant. The intercept for equation (1a) may imply that further oxidation pathway(s) are taking place in the smaller aerosol that operates independently of initial buffering capacity, as suggested by *Vogt et al.* [1996]. Furthermore, the R^2 of 0.80 could indicate that a minority of the NSS production may be by these further oxidation pathways. These pathways do not appear significant for the coarse aerosol, although this is not surprising in light of the relative reaction rates of O_3 oxidation [*Chameides and Stelson*, 1992] versus those proposed by *Vogt et al.* [1996]. Consideration of the standard error of the regression coefficient indicates a 90% CI for buffering capacity to be in the range 1.6 to 2.4 times Alk. Such a large enhancement of Alk. requires further explanation.

O_3 oxidation of SO_2 in SSAW was considered by *Artaxo et al.* [1992] to be an important contributor to the observed $CaSO_4$. They attributed much of the CaX found to be of biogenic origin (mostly as $CaCO_3$) and noted that substantially more $CaSO_4$ was observed in aerosols during summertime, supporting the hypothesis of a biogenic $CaCO_3$ source for the sulfur in these aerosols. Further, the strong presence of non-soil-derived $CaSO_4$ in sea-salt aerosols was argued to result mainly from enhanced O_3 oxidation of SO_2 to $CaSO_4$ in the Ca^{++} and $CO_3^=$ enriched SSAW (from dissolved $CaCO_3$). Since $CaCO_3$ provides added carbonate buffering, O_3 oxidation of SO_2 can be maintained after all aerosol alkalinity has been consumed.

Individual particle analysis by SEM-X-ray (J. Anderson, personal communication, June 1997) showed there to be non-soil-derived $CaSO_4$ aerosols present in Cape Grim samples. On a number basis, 3-5% of the over 50,000 particles analyzed contained non-soil-derived $CaSO_4$. The size distribution data from SEM analysis indicate 5-10% on a mass basis of the total particles contained this $CaSO_4$. There is also evidence from SEM analysis that biogenic $CaCO_3$ fragments were present in sea-salt aerosols.

Figure 3 shows a TEM image of an ~ 0.8 μm dry (about 1.5 μm ambient) diam sea-salt aerosol particle having mixed-cation sulfate, SiO_2 (given its shape and character, not soil-derived, but likely an algal fragment), and calcite ($CaCO_3$ in the coccolith fragment on the right in Figure 3) determined by electron diffraction analysis [*Posfai et al.*, 1995]. Analysis of the whole particle produced the following atomic percent ratios relative to Na: Ca, 0.25; Mg, 0.17; S, 0.082; K, 0.024; and Cl, 1.04. Assuming all the S is as sulfate (2-3% may actually be MSA), these ratios relative to seawater ion concentration are 11.5 (Ca^{++}); 1.50 (Mg^{++}); 1.36 ($SO_4^=$); 1.09 (K^+); 0.89 (Cl^-). Much of the 1150% Ca enrichment for this particle is complemented by

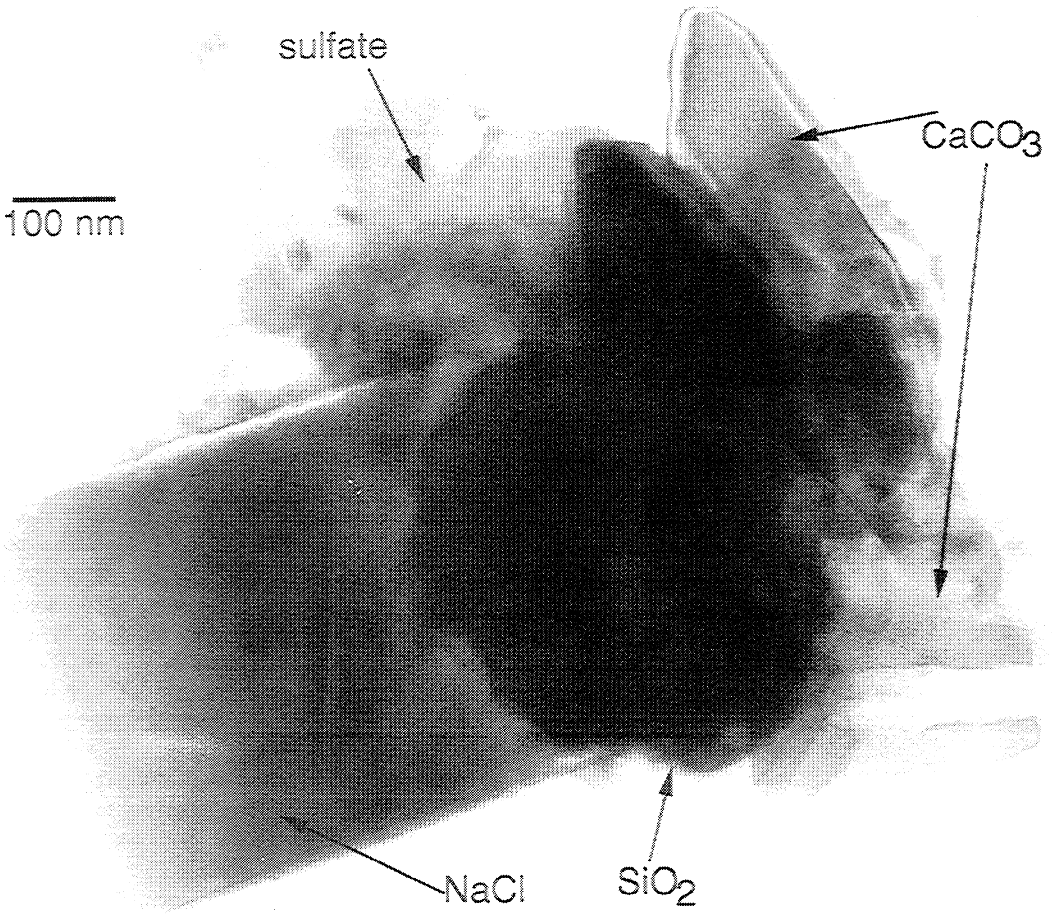

Figure 3. Transmission electron microscope image of a sea-salt aerosol particle consisting of NaCl, mixed-cation sulfate, SiO_2 (probably an algal fragment), and calcite, $CaCO_3$ (as confirmed by EDS and electron diffraction). The morphology of this calcite is indicative of a coccolith fragment.

carbonate ($CO_3^=$) in the coccolith fragment. Many extremely small fragments, for example, due to broken coccolith rib fragments (lower right in Figure 3) further reduced in size by wave action, can readily be dissolved to produce $CO_3^=$ buffering [*Bradshaw and Brewer*, 1988]. Perhaps this is why $SO_4^=$ in the pictured particle is enriched 2 to 3 times over that of the bulk 0.9-2.3 μm diam aerosol NSS enrichment. We cannot conclude from the Figure 3 example particle nor even from the remaining data described above that all of the CaX found at Cape Grim during ACE 1 is due to biogenic $CaCO_3$ fragments. However, the majority may well have been so derived. This could easily lead to carbonate buffering capacity increases of 50% and more for Cape Grim conditions, and of 100% and more for ship transit conditions (see Table 3).

Given the above discussion, a surrogate measure of the maximum total sea-salt aerosol buffering capacity is the equivalence sum of aerosol alkalinity and non-soil-derived CaX. Note that a portion of this buffering capacity, about 0.2 neq m^{-3}, may be associated with the fine and very fine aerosols under the high wind speed conditions of ACE 1 (see Table 3). The equivalence sum of Alk. and CaX values suggests that the total sea-salt aerosol buffering capacity was 1.8 times that of bulk seawater alkalinity alone. This compares favorably with the 1.6 to 2.4 ratio of buffering capacity to Alk. derived from the regression analysis results, equations (1a) and (1b).

If we consider the equivalence sum of Alk. and CaX as being a maximum bound on buffering capacity, then up to 90% of the NSS in coarse aerosols may be attributed to O_3 oxidation of SO_2 in SSAW. As a minimum estimate of this attribution, we use the 99% confidence low bound slope from equation (1b) of 1.42. This results in at least 70% of the coarse NSS being attributed to O_3 oxidation of SO_2 in SSAW. Thus 70-90% of the NSS in coarse aerosols may be attributed to O_3 oxidation of SO_2 in SSAW. The buffering capacity enhancement factor which may apply to any one region of the MBL depends on meteorological parameters such as wind speed, temperature, and RH, and probably more so that region's biological productivity which controls biogenic material and chemical enhancement in the surface microlayer. This is evident in the ship transit aerosol data of Table 3.

Size dependent oxidation in SSAW has not yet been discussed. A comparison of observed versus predicted NSS by size was considered in the modeling analysis of *Gurciullo et al.* [this issue]. For the four Sierra supermicron size ranges, 0.9-2.3, 2.3-4.5, 4.5-8, and 8-16 μm ambient diam, all of the observed NSS in the two largest size ranges, 0.32 nmol m^{-3} (4.5-8 μm) and 0.10 nmol m^{-3} (8-16 μm) can be attributed to oxidation in SSAW. A substantial majority of the 0.21 nmol NSS m^{-3} in the 2.3-4.5 μm range is due to oxidation in SSAW. The combination of oxidation in SSAW and cloud processing is required to explain the 0.28 nmol NSS m^{-3} in the 0.9-2.3 μm range.

The Cape Grim seasonal NSS data of Table 2b indicate that average spring and summer coarse NSS are 20-30% greater than that observed during ACE 1. Buffering capacity (and conversion rates) may be enhanced during spring and summer as a whole compared to that which prevailed during ACE 1. The coarse and fine NSS of 1.48 and 0.34 nmol m^{-3}, respectively, during the austral winter season (June, July, August) are to be noted. Greater wind speeds, especially the 45% occurrence of >11 m s^{-1} wind speeds [*Jasper and Downey*, 1990], causes more alkalinity to be present in coarse sea-salt aerosols compared with spring and summer. The magnitude of alkalinity in fine sea-salt aerosols is also enhanced over that in spring and summer since smaller sea-salt aerosols are, relatively, more enhanced under very high wind speeds. *O'Dowd et al.* [1997] indicate that the number of film drops (of mean diam 0.4 μm, $\sigma = 1.9$) produced by the bubble-bursting process increases from 13-14 cm^{-3} at 9 m s^{-1} to 32-35 cm^{-3} at 13 m s^{-1} and 50-55 cm^{-3} at 15 m s^{-1} wind speeds. Thus buffering capacity of 2 neq m^{-3}, and more, in coarse aerosols and up to 0.1 neq m^{-3} in fine may be available. This would provide sufficient buffering to allow O_3 oxidation of SO_2 in SSAW to explain at least 70% of the 1.48 nmol NSS m^{-3} found in coarse and 20-30% of the 0.34 nmol NSS m^{-3} found in fine aerosols at Cape Grim during winter.

On the basis of the above arguments, and given that (4-14) x 10^{15} g yr^{-1} of sea salt cycles through the global atmosphere [*Monahan*, 1986; *Gong et al.*, 1997], the buffering capacity flux which may be brought into the atmosphere annually is from 4 x 10^{11} eq to as much as 20 x 10^{11} eq. This is based on the buffering capacity flux being up to 5/3 the bulk seawater alkalinity flux. Assuming this buffering capacity to equal the SO_2 converted by O_3 oxidation in SSAW, (2-10) x 10^{11} mol yr^{-1} of SO_2 is annually converted by this mechanism to NSS. *Chameides and Stelson* [1992] had estimated (1-4) x 10^{11} mol yr^{-1} for this SO_2 sink in the MBL; they concluded that this sink may vie with in-cloud oxidation for the removal of SO_2 in the remote MBL. The estimation presented here suggests O_3 oxidation in SSAW may be a greater sink for SO_2 than in-cloud oxidation in the remote MBL. However, we note that it is presently not possible to state by how much the biogenic, surface microlayer source contributes on a global basis to buffering capacity in the MBL.

An analysis of in-cloud oxidation of SO_2 by *Lelieveld* [1993] concluded that (8-20) x 10^{11} mol yr^{-1} is removed from the atmosphere as a whole by in-cloud oxidation. The O_3 oxidation in SSAW pathway for SO_2 removal is of the same order as this magnitude. For some regions of the MBL, such as shown by *Yvon and Saltzman* [1996], more SO_2 can be lost from the atmosphere due to O_3 oxidation in SSAW than from homogeneous and in-cloud oxidation combined. One may ask whether this, perhaps, dominant pathway for the removal of SO_2 from the remote MBL still allows for reasonable SO_2 residence times. For the ACE 1 setting, a median MBL residence time for SO_2 with respect to O_3 oxidation in SSAW may be determined using $[SO_2]$ of 14 pptv [*DeBruyn et al.*, 1998], an MBL height of 700 m [*Hainesworth et al.*, 1998; *Russell et al.*, 1998], the 0.7-0.9 nmol NSS m^{-3} attributed here to O_3 oxidation in SSAW, and an NSS deposition velocity of 0.7 cm s^{-1} [*Slinn and Slinn*, 1980; *Williams*, 1982; *Sievering*, 1984]. The result is a median residence time with respect to O_3 oxidation in SSAW of 21 hours; considering uncertainty, it could be no less than 10 hours. Indeed, this is a reasonable value when compared to sea-salt aerosol residence times of 20-40 hours during ACE 1.

5. Conclusions

Of the total 2.2-2.3 nmol NSS m^{-3} observed at 110-130 m asl at Cape Grim, 0.7-0.9 nmol m^{-3} or about 35% has been attributed to O_3 oxidation of SO_2 in SSAW. Further, the amount of NSS produced by this mechanism in the MBL during the ACE 1 remote Southern Ocean experiment vied with that produced by homogeneous and cloud conversion. From 70% to as much as 90% of the NSS found in >0.7 μm diam coarse sea-salt aerosols is attributed to O_3 oxidation. The remaining coarse aerosol NSS may have been contributed by other sea-salt aerosol conversion mechanisms and/or by cloud production and processing.

The conclusion that about 35% of the total NSS observed in the MBL during ACE 1 may be attributed to O_3 oxidation of SO_2 in SSAW incorporates the observation that sea-salt aerosol buffering capacity was enriched about 50-100% over bulk seawater alkalinity (Alk.). This may be partly due to aerosol alkalinity being greater than Alk. resulting from the shifting thermodynamic equilibrium of CO_2 as the sea-salt aerosol evolves, but more so from added carbonate due to biogenic material in the surface microlayer. Chemical modification of sea-salt aerosols is thus prevalent not only in the polluted MBL but also in the remote MBL. Since chemically unmodified sea-salt aerosols introduce a global and annual average radiative forcing of about -2 W m^{-2} (more in climates with strong winds [*Winter and Chýlek*, 1997] such as was true during ACE 1), the negative forcing due to chemically modified sea-salt aerosols may be of added importance to Earth's radiation balance through modification of aerosol optical properties (Y. Kim, personal communication, October 1997).

Modification of the sulfur cycle in the MBL by O_3 oxidation of SO_2 in SSAW may have other more important implications. Because a substantial fraction of the dimethylsulfide emitted by marine organisms is converted to SO_2 in the MBL, the added NSS dry deposition removal in coarse SSAW-laden aerosols (which reduces NSS residence time in the MBL) may markedly reduce the feedback between greenhouse warming, oceanic dimethylsulfide emissions, and sulfate haze albedo.

Acknowledgments. We would like to state our appreciation for the support of Director Chad Dick and his Cape Grim Observatory staff, especially in helping us obtain data from the 50-m tower level. We want to thank P. Quinn and M. Hamilton of NOAA-PMEL, as well as A. Pszenny of MIT, for their help with *Discoverer* cascade impactor sampling. We also thank J. Ivey and others of the Australian Government Analytical Laboratory for IC analysis. Finally, we wish to thank W. Keene of the University of Virginia and A. Pszenny of MIT for useful comments on the manuscript. This research was funded by NSF grants ATM-9419418 and ATM-940874. It is a contribution to an International Global Atmospheric Chemistry (IGAC) Core project of the IGBP as well as being a part of the IGAC Aerosol Characterization Experiments (ACE).

References

Andreae, M., R. Charlson, F. Bruynseels, H. Storms, R. van Grieken, and W. Maenhaut, Internal mixture of sea salt, silicates and excess sulfate in marine aerosols, *Science, 232*, 1620-1622, 1986.

Artaxo, P., M. Rabello, W. Maenhaut, and R. van Grieken, Trace elements and individual particle analysis of atmospheric aerosols from the Antarctic peninsula, *Tellus, Ser. B; 44B*, 318-334, 1992.

Ayers, G.P., and J. Gras, The concentration of Ammonia in Southern Ocean air, *J. Geophys. Res., 88*, 10655-10659, 1983.

Ayers, G.P., and T. Larson, Numerical study of droplet size dependent chemistry in oceanic, wintertime stratus cloud at southern mid-latitudes, *J. Atmos. Chem., 11*, 143-167, 1990.

Baines, P., and D. Murray, Modeling of the airflow over Cape Grim, *Baseline 92*, pp. 20-24, available from CSIRO Div. Of Atmos. Res., Aspendale, Victoria and Australia, 1992. Berresheim, H., A. Andreae, G. Ayers, R. Gillette, J. Merrill, V. Davis, and W. Chameides, Airborne measurements of DMS, SO_2, and aerosol ions over the Southern Ocean south of Tasmania, J. Atmos. Chem., 10, 341-370, 1990.

Bezdek, H., and A. Carlucci, Concentration of and removal of liquid microlayers from a seawater surface by bursting bubbles, *Limnol. Oceanogr., 19*, 126-132, 1974.

Bradshaw, A., and P. Brewer, High precision measurements of alkalinity and total carbon dioxide in seawater by potentiometric titration, *Mar. Chem., 23*, 69-86, 1988

Cainey, J., The atmospheric sulfur cycle in the remote Southern Ocean environment, Ph.D. thesis, Monash Univ., Clayton, Victoria, Australia, 1997.

Cattell, F., W. Scott, and D. du Cros, Chemical composition of aerosol particles greater than 1-μm diameter in the vicinity of Tasmania, *J. Geophys. Res., 82*, 3457-3462, 1977.

Chameides, W.L., and A.W. Stelson, Aqueous-phase chemical processes in deliquescent sea-salt aerosols: A mechanism that couples the atmospheric cycles of S and sea salt, *J. Geophys. Res., 97*, 20565-20580, 1992.

Davis, D., Aircraft ammonia measurements during ACE 1, paper presented at San Francisco, Calif., Air-Sea Exchange Session, Fall 1997 American Geophysical Union Meeting, San Francisco, Calif., Dec. 11, 1997.

DeBruyn, W. J., T. Bates, and E. Saltzman, Shipboard measurements of dimethylsulfide and sulfur dioxide southwest of Tasmania, *J. Geophys. Res., 103*, 16703-16712, 1998.

Downey, A. and J. O. Jasper, Cape Grim climatology, *Baseline 95*, pp. 92-98, CSIRO Div. of Atmos. Res., 1996.

Duce, R., and E. Hoffman, Chemical fractionation at the air/sea interface, *Ann. Rev. Earth Planet. Sci., 3*, 187-228, 1976.

Gong, S. L., L. Barrie, J. Prospero, D. Savoie, G. Ayers, and J. Blanchette, Modeling sea-salt aerosols in the atmosphere: Atmospheric concentrations and fluxes, *J. Geophys, Res., 102*, 3819-3830, 1997.

Gravenhorst, G., Maritime sulfate over the North Atlantic, *Atmos. Environ., 2*, 707-713, 1978.

Gurciullo, C., B. Lerner, H. Sievering, and S. Pandis, Heterogeneous sulfate production in the remote marine environment: Cloud processing and sea-salt particle contributions, *J. Geophys. Res.*, this issue.

Hainsworth, A., A. Dick, J. and Gras, Climatic context of the First Aerosol Characterization Experiment(ACE 1), *J. Geophys. Res., 103*, 16319-16340, 1998.

Henrichs, S., and P. Williams, Dissolved and particulate amino acids and carbohydrates in the sea surface microlayer, *Mar. Chem., 17*, 141-163, 1985.

Hoffman, E., and R. Duce, Factors influencing the organic carbon content of marine aerosols: a laboratory study, *J. Geophys. Res., 81*, 3667-3670, 1976.

Hoppel, W., G. Frick, J. Fitzgerald, and B. Wattle, A cloud chamber study of the effect that clouds have on the aerosol size distribution, *Aerosol Sci. Technol, 20*, 1-30, 1994.

Jasper, J.A., and A. Downey, Cape Grim Climatology, *Baseline 90*, pp. 59-61, *CSIRO Div. of Atmos. Res.*, 1990.

Junge, C.E., Our knowledge of the physico-chemistry of aerosols in the undisturbed marine environment, *J. Geophys. Res., 77*, 5183-5200, 1972.

Keene, W.C., R. Sander, A. Pszenny, R. Vogt, P. Crutzen, and J. Galloway, Aerosol *p*H in the marine boundary layer, *J. Aerosol Sci., 29(3)*, 339-356, 1998.

Kim, Y., H. Sievering, and J. Boatman, Volume and surface area size distribution, water mass and model fitting of CASE-WATOX marine aerosols, *Global Biogeochem. Cycles, 4*, 165-177, 1990.

Kim, Y., H. Sievering, J. Boatman, D. Wellman, and A. Pszenny, Aerosol size distribution and aerosol water content measurements during the Azores Marine Aerosol and Gas Exchange Experiment, *J. Geophys. Res., 100*, 23061-23067, 1995.

Lelieveld, J., Multi-phase processes in the atmospheric sulfur cycle, *in Interactions of C, N, P, and S Biogeochemical Cycles and Global Change, NATO ASI Ser.*, vol. 14, edited by R. Wollast, F., Mackenzie, and L. Chou, pp. 304-327, Springer-Verlag, New York, 1993.

Lowe, J., M. Smith, C. O'Dowd, and S. Clegg, The effects of sea salt aerosol on the production of sulphate in the MBL and its effect on stratiform clouds, *ICCP Proc .9*, 1195-1199, 1996.

Luria, M., and H. Sievering, Heterogeneous and homogeneous oxidation of SO_2 in the remote marine atmosphere, *Atmos. Environ., Part A, 25*, 1489-1496, 1991.

MacIntyre, F., Chemical fractionation and sea-surface microlayer processes, *Sea, 5*, 245-299, 1974.

Maenhaut, W., H. Raemdonck, A. Selen, R. van Grieken, and J. Winchester, Characterization of the atmospheric aerosol over the eastern equatorial Pacific, *J. Geophys. Res., 88*, 5353-5364, 1983.

Millero, F., Thermodynamics of the carbon kinetic system in the oceans, *Geochim. Cosmochim. Acta, 59*, 661-677, 1995.

Monahan, E.C., The ocean as a source for atmospheric particles, in *The Role of Air-Sea Exchange in Geochemical Cycling, NATO ASI Ser.*, edited by P. Guat-Menard, pp. 129-169, D. Reidel, Norwell, Mass., 1986.

Noone, K., E. Ostrom, R. Pockalay, and R. Van Grieken, Chemical and microphysical properties of cloud droplet residual particles in marine stratocumulus clouds observed during the MAST experiment, *ICCP Proc. 9*, 1175-1177, 1996.

O'Dowd, C., M. Smith, I. Consterdine, and J. Lowe. Marine aerosol, sea-salt, and the marine sulphur cycle: a short review, *Atmos. Environ., 31*, 73-80, 1997.

Posfai, M., J. R. Anderson, P. Buseck, and H. Sievering, Compositional variation of sea-salt mode aerosol particles from the North Atlantic, *J. Geophys. Res., 100*, 23063-23074, 1995.

Prospero, J. M. and D. Savoie, AEROCE scientific results 1988-1992, Rosenthiel Sch. of Mar. and Atmos. Sci., Univ. of Miami, Miami, Fla., 1993.

Quinn, P. K., D. Coffman, V. Kapustin, T. Bates, and D. Covert, Aerosol optical properties in the MBL during ACE 1 and the underlying chemical and physical aerosol properties, *J. Geophys. Res., 103*, 16547-16564, 1998.

Russell, L., D. Lenschow, K. Laursen, T. Bates, A. Bandy, D. Thornton and S. Siems, Bidirectional mixing in an ACE 1 MBL overlain by a second turbulent layer, *J. Geophys. Res., 103*, 16411-16432, 1998.

Sievering, H., Small-particle dry deposition on natural waters: modeling uncertainty, *J. Geophys. Res., 89*, 9679-9681, 1984.

Sievering, H., G. Ennis, E. Gorman, and C. Nagamoto, Heterogeneous sulfur conversion in sea salt aerosol particles: Size distribution and statistical analysis of nitrate, excess sulfate, and chloride deficit in the marine boundary layer during GCE/CASE/WATOX, *Global Biogeochem. Cycles, 4*, 395-406, 1990.

Sievering, H., J. Boatman, J. Galloway, W. Keene, Y. Kim, and M. Luria, Heterogeneous sulfur conversion in sea-salt aerosol particles: The role of aerosol water content, and size distribution, *Atmos. Environ., Part A, 25*, 1479-1487, 1991.

Sievering, H., J. Boatman, E. Gorman, Y. Kim, L. Anderson, G. Ennis, M. Luria, and S. Pandis, Removal of sulfur from the marine boundary layer by ozone oxidation in sea-salt aerosol, *Nature, 360*, 571-574, 1992.

Sievering, H., J. Boatman, E. Gorman, T. Ley, A. Pszenny, and Y. Kim, Ozone oxidation of sulfur in sea-salt particles during the Azores Marine Aerosol and Gas Exchange Experiment, *J. Geophys. Res., 100*, 23075-23081, 1995.

Slinn, S. A., and W. Slinn, Predictions for particle deposition on natural waters, *Atmos. Environ., 14*, 1013-1016, 1980.

Tseng, R. S., R. Skop, and J. Brown, Sea-to-air transfer of surface-active organic compounds by bursting bubbles, *J. Geophys. Res., 97*, 5201-5206, 1992.

Vogt, R., P. Crutzen, and R. Sander, A mechanism for halogen release from sea-salt aerosol in the remote marine boundary layer, *Nature, 383*, 327-330, 1996.

Warneck, P., *Chemistry of the Natural Atmosphere*, 757 pp., Academic, San Diego, Calif., 1988.

Wedding, J., A. McFarland, and J. Cermak, Large particle collection characteristics of ambient aerosol samples, *Environ. Sci. Technol, 11*, 387-390, 1977.

Wexler, A.S., and J.H. Seinfeld, The distribution of ammonium salts among a size and composition dispersed aerosol, *Atmos. Environ., Part A, 24*, 1231-1246, 1990.

Wexler, A.S.,and J.H. Seinfeld, Second-generation inorganic aerosol model, *Atmos. Environ., Part A, 25*, 2731-2748, 1991.

Williams, R. M., A model for the dry deposition of particles to natural water surfaces, *Atmos. Environ., 16*, 1933-1938, 1982.

Winkler, P., Sea-salt aerosol *p*H and water, in *Chemistry of Multiphase Atmospheric Systems* edited by W. Jaeschke, pp. 269-298, Spring, Heidelberg, 1986.

Winter, B., and P. Chýlek, Contribution of sea salt aerosol to the planetary clear-sky albedo, *Tellus, Ser. B, 49*, 72-79, 1997.

Yvon, S.A., and E.S. Saltzmann, Atmospheric sulfur cycling in the tropical Pacific marine boundary layer, *J.Geophys. Res., 101*, 6911-6918, 1996.

J. Anderson and M. Posfai, Department of Geology and Chemistry, Arizona State University, Tempe, AZ 85287.

J. Cainey, CSIRO Atmospheric Research, Aspendale, Victoria, Australia.

B. Lerner, H. Sievering (corresponding author), and J. Slavich, CB 172, Global Change and Environmental Quality Program and Department of Environmental Sciences and Geography, University of Colorado at Denver, P.O. Box 173364, Denver, CO 80217-3364. (hsieveri@carbon.cudenver.edu)

(Received July 7, 1998; revised November 20, 1998; accepted November 30, 1998.)